Eur. Phys. J. B **40**, 11–17 (2004)
DOI: 10.1140/epjb/e2004-00233-7

THE EUROPEAN PHYSICAL JOURNAL B

# Room temperature metal–insulator transition in as grown $(La_{1-x}Sr_x)_yMnO_3$ thin films deposited by molecular beam epitaxy

A.Yu. Petrov[1], C. Aruta[1,a], S. Mercone[1], C. Adamo[1], I. Alessandri[2], and L. Maritato[1]

[1] INFM "Coherentia" and INFM-UdR di Salerno Dipartimento di Fisica, Università di Salerno, Italy
[2] INSTM, Laboratorio di Strutturistica Chimica, Dipartimento di Ingegneria Meccanica, Università di Brescia, Italy

Received 12 March 2004 / Received in final form 6 June 2004
Published online 3 August 2004 – 

**Abstract.** We have fabricated by an in situ process $(La_{1-x}Sr_x)_yMnO_3$ epitaxial thin films by Molecular Beam Epitaxy using a low partial pressure ($\cong 2 \times 10^{-5}$ torr) of $O_2$+5% ozone. Reflected High Energy Electron Diffraction analysis has been performed during the growth process to check the structural properties of the films. The samples have not been subjected to any in situ or ex situ post deposition annealing procedure. Thin films on different substrates ($SrTiO_3$, $LaAlO_3$, $NdGaO_3$) and with different thickness have been fabricated to compare the transport properties and investigate the effects of the epitaxial strain. For compositions around $x = 0.3$, Metal-Insulator (MI) transitions at temperature as high as $T_{MI} = 340$ K have been observed in thin films few nanometers thick. Resistivity versus temperature curves measured on samples deposited in the same run onto different substrates, have shown clear effects related to the epitaxial strain. These results are very promising for a deeper understanding of the physical mechanisms at work in manganites and in view of the future fabrication of manganite-based heterostructures for electronic applications.

**PACS.** 75.47.Lx Manganites – 81.15.Hi Molecular, atomic, ion, and chemical beam epitaxy

## 1 Introduction

The room temperature Colossal MagnetoResistance (CMR) manganites, with chemical formula $La_{1-x}A_xMnO_3$ (A=Ca, Sr, Ba) have been extensively studied in the last years, for their interesting physical properties also in view of several possible applications. Thin films of these compounds have been produced and investigated to analyse the dependence of their magnetotransport properties on different physical parameters [1]. The subtle interplay of the spin, charge and orbital degrees of freedom operating in manganites, causes their phase diagrams to be extremely rich and appealing for many studies and applications. As an example, the strong electron-phonon coupling mediated by the Jahn-Teller distortion of the $MnO_6$ octahedra, is expected to make manganites extremely sensitive to the hydrostatic pressure and to the substrate-induced biaxial strain [2], opening the door to the possibility of controlling their magnetotransport properties via the choice of suitable substrates and thicknesses. A large amount of studies about this issue has been performed on manganite epitaxial thin films and seemed to confirm this possibility [3]. However, the main role of biaxial strain in determining the magnetotransport properties of the manganite thin films has been recently questioned [4], indicating other parameters such as the actual doping level and the presence of cation vacancies, to play a major role. Therefore, in order to compare the performances of manganite thin films with different epitaxial strain, it is critical to deal with identical samples, to avoid the presence of spurious effects that can hide the investigated mechanisms.

More generally, in the case of manganites, the intimate correlation among the many parameters determining their properties and the richness of their phase diagrams, poses a strong demand on the accurate control of the samples characteristics. A careful monitoring of structural and compositional properties of manganite thin films is fundamental to discriminate about the role played by different parameters, in order to determine the actual physical properties and in view of possible microelectronic applications.

Different physical vapour deposition techniques (Pulsed Laser Ablation (PLD), Sputtering, Molecular Beam Epitaxy (MBE)) have been successfully used to fabricate manganite films [5] with epitaxial structural properties and high Curie temperatures (above room temperature).

Unfortunately, the most used deposition techniques (PLD and Sputtering), are able to produce high quality manganite thin films only by introducing in the deposition

[a] e-mail: aruta@sa.infn.it

chamber oxygen partial pressures higher than $10^{-3}$ torr and thus preventing the use of in situ structural analysis such as RHEED (Reflected High Energy Electron Diffraction). Moreover, manganite thin films are often subjected to an in situ, post deposition annealing procedure at high temperature (around 900 °C) in the presence of even higher (up to one atmosphere) oxygen pressures, to obtain optimal magnetotransport performances [6]. This annealing process poses severe limitation to the production of electronic devices where very thin layers are needed or where different layers of manganite materials have to be deposited without interface interdiffusion.

MBE technique has proved to be able to produce as grown epitaxial manganite thin films with optimal magnetotransport properties, without any post deposition annealing. In MBE deposition process, low partial pressures ($10^{-6}$–$10^{-5}$ torr) of pure ozone are employed, allowing the real time control of structural properties of growing samples by RHEED [7]. On the other hand, ozone is a very hazardous gas which is highly corrosive and needs particular care in the handling [8].

In this work, we report about the MBE fabrication of $(La_{1-x}Sr_x)_yMnO_3$ epitaxial thin films deposited at a low partial pressure ($\cong 2 \times 10^{-5}$ torr) of $O_2$+5% ozone. RHEED analysis were performed during the growth process to check the structural properties of the films. As grown epitaxial manganite thin films, few tens of nanometers thick, have shown Metal-Insulator (MI) transitions at temperature as high as $T_{MI} = 340$ K, without any post deposition annealing. The magnetotransport properties of thin films deposited on different substrates have also been measured and compared. The obtained results are very promising for a better discrimination of the role played in the physical properties by many different parameters, and in particular by the epitaxial strain, and in view of future possible applications of manganite thin films in microelectronics.

## 2 Experimental

We deposited $(La_{1-x}Sr_x)_yMnO_3$ epitaxial thin films by MBE using a codeposition procedure in which the elemental rates of La (e-beam evaporated), Sr and Mn (effusive cells evaporated) were carefully controlled to obtain the desired sample composition. Typical total deposition rates were around 0.1 Å/s. A substrate temperature of about 700 C° and a low partial pressure ($\cong 2 \times 10^{-5}$ torr) of $O_2$+5% ozone were used. The mixture of $O_2$+5% ozone gas was obtained using a commercial ozonizer, which does not require any particular care in the handling. All the pipelines and the valves connecting the ozonizer to the deposition chamber were made of teflon and stainless steel. A mass spectrometer controlled the atmosphere composition inside the deposition chamber. The growth process were monitored by RHEED analysis. Samples on different $5 \times 5$ mm$^2$ substrates ($SrTiO_3$ (100) (STO), $LaAlO_3$ (100) (LAO) and $NdGaO_3$ (110) (NGO) single crystals) and with different thickness have been grown. The substrate compounds have a perovskite structure (or a distorted one in the case of NGO), which matches quite well the structure of $La_{0.7}Sr_{0.3}MnO_3$ compound with pseudo-cubic bulk value 3.873 Å. STO and LAO are cubic with respectively $a = 3.905$ Å and $a = 3.788$ Å and NGO is orthorhombic with pseudocubic lattice parameters $a = 3.862$ Å and $c = 3.854$ Å. All the substrates were simultaneously introduced in the deposition chamber and were positioned very close to each other on the heated sample-holder to avoid spread in the composition of the films. A (100) MgO single crystal substrate was also used to carry out compositional analysis after the deposition. The cationic stoichiometry of the samples was controlled by Energy Dispersive Spectroscopy (EDS) analysis in a Scanning Electron Microscope (SEM). X-ray Diffraction (XRD) analysis has been performed on the produced samples after the deposition to characterize their crystal properties. The XRD measurements have been carried out at Cu K$\alpha$ energy by using a standard two-axes diffractometer in Bragg-Brentano focusing geometry (Rigaku D/MAX-6). A third axis, allowing for the rotation of the samples around their surface normal, was also present. X-Ray Reflectivity (XRR) measurements have been carried out by a Bruker D8 diffractometer equipped with a Göbel mirror. The transport behaviour of the samples at different temperatures has been measured using a standard four probe geometry.

## 3 Results

The low partial pressure ($\cong 2 \times 10^{-5}$ torr) of $O_2$+5% ozone present in the vacuum chamber during the deposition, allowed the growth monitoring of the films by RHEED analysis. Perfectly planar thin films, with surface roughness of the order of the interatomic distances, are in principle expected to show sharp spotty RHEED patterns, related to the intercepts of the reciprocal lattice rods with the Ewald sphere. In actual experimental set up, the finite thickness of the Ewald sphere and the diffusion of the reciprocal rods can result in streaky RHEED patterns. The presence of bulbous, somewhat diffuse, streaks patterns can also be related to short in-plane coherence [9]. The RHEED pattern shown in Figure 1a, for a typical $(La_{1-x}Sr_x)_yMnO_3$ film deposited on STO, presents well defined streaks and can be associated to the growth of thin films with surface roughness of the order of the interatomic distances [10]. Moreover, in the inset to Figure 1a, the oscillations in the intensity of the RHEED reflected spot during the deposition process are shown. Each of these oscillations is related to the deposition of an atomic monolayer, allowing to control in real time the growth rate [11]. The final thickness of the samples was varied by changing the total deposition time. In some films, the streaky RHEED pattern, probably because of undesired fluctuations in the deposition conditions, was lost after the first minutes of growth and a spotty pattern, as shown in Figure 1b, associated to a surface roughness higher than the interatomic distances, appeared.

After the growth process was completed, the partial pressure of $O_2$+5% ozone in the deposition chamber was

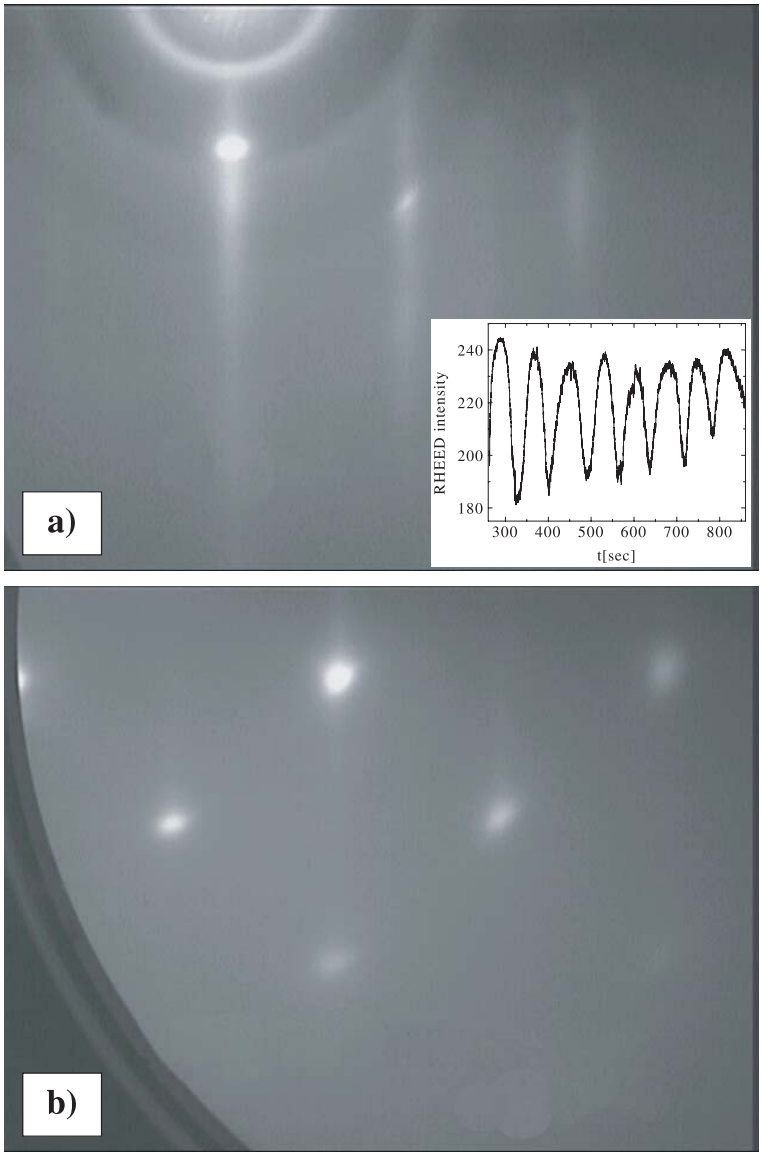


**Fig. 1.** a) RHEED image of a typical $(La_{1-x}Sr_x)_yMnO_3$ thin films on STO. Streaks are clearly visible, indicating an atomically flat surface of the investigated sample. Inset: Oscillations of the RHEED reflected spot. b) RHEED image measured on a $(La_{0.7}Sr_{0.3})_{0.9}MnO_3$ thin film deposited on STO. In this case, the presence of spots is associated to a surface roughness higher than the typical interatomic distances.

kept constant at the value of $2\times10^{-5}$ torr until the temperature of the substrates reaches 100 C° (typically in about 30 minutes). The introduction of the low percentage of ozone gas in the chamber during the fabrication process, did not give appreciable signs of extra corrosion on the most exposed parts of the MBE system (hot filaments, effusive cells, e-beam crucible, heated sample holder). No particular care was taken in handling and storing the produced samples in air.

Due to the employed deposition process which uses a different source for each element to evaporate, the ratio between the stoichiometries of La+Sr and Mn, as controlled by EDS analysis, was generally different from 1. Therefore we quote the chemical formula of our thin films as $(La_{1-x}Sr_x)_yMnO_3$. Obviously, when $y$ is different from 1, the hole doping level of the system is related not only to the value of $x$ but also to the actual oxygen stoichiometry which plays an important role in the carrier concentration [12]. The charge neutrality request allows, in principle, the determination of the oxygen content by knowing $x$ and $y$ from the EDS analysis. On the other hand, the accurate determination of the oxygen in thin film samples is always very difficult and, moreover, the low accuracy (around 5%) in the EDS measurements, imposes some

uncertainty on the actual value of $x$ and $y$. In spite of these limitations, we have generally found a correlation among the properties of the produced thin films and the compositional values, as determined by EDS, in good agreement with previous data present in literature [13].

Small angle XRR measurements confirmed the perfect planarity of the films. In Figure 2a, XRR spectrum for a $(La_{0.7}Sr_{0.3})_{0.6}MnO_3$ thin film deposited on STO is shown. From the period of the oscillations, a total thickness of 448 Å is estimated, with a surface roughness of 4 Å, of the same order of magnitude as the interatomic distances in manganites. This result is in agreement with the RHEED analysis performed during the deposition procedure. Reflectivity measurements carried out on films deposited for shorter time, (Fig. 2b), showed similar results for the surface roughness, with total thickness in the range of few nanometers (60–90 Å). X-ray specular theta-2theta diffraction analysis indicated perfectly epitaxial thin films, with peaks in the spectra only coming from the $(00l)$ reflections of the substrate and the thin film lattices. By using asymmetric diffraction, the in-plane film lattice parameters were found practically identical to those of the used substrates. Film specular reflections were very close to those of the substrate and with a very low intensity. However, when the determination of the out-of plane lattice parameter was possible, it resulted elongated or shortened with respect to the bulk values, in agreement with the in-plane lattice strain induced by the substrate. In fact, $La_{1-x}Sr_xMnO_3$ epitaxial thin films, with composition close to $x \cong 0.3$, are known to grow with tensile strain on STO substrates, with compressive strain on LAO and almost without strain on NGO [3,14]. Consequently, $La_{0.7}Sr_{0.3}MnO_3$ compound grown in form of thin films does not exhibit a rhombohedral cell as in the bulk form [15] but a tetragonal one [16]. Moreover, the strength of the strain is generally related to the lattice mismatch between the substrate and the bulk material to be deposited. If we define the in-plane lattice mismatch by $m = (a_{\text{substrate}} - a_{\text{bulk}})/a_{\text{substrate}}$, in the case of $La_{0.7}Sr_{0.3}MnO_3$ on STO $m$ is equal to $+0.81\%$ (+ indicating in-plane tensile strain), while for $La_{0.7}Sr_{0.3}MnO_3$ on LAO $m = -2.2\%$ (– being associated to in-plane compressive strain) [17]. Therefore, we expect to observe values of the out-of-plane $La_{0.7}Sr_{0.3}MnO_3$ lattice parameter slightly smaller than the pseudo-cubic bulk value (3.873 Å) [17] for films deposited on STO and larger than the bulk for films on LAO. In Figure 3, XRD spectra for $(La_{0.7}Sr_{0.3})_{1.3}MnO_3$ films, deposited on LAO (Fig. 3a) and NGO (Fig. 3b), are shown. Both films were grown together during the same deposition run and their thickness, (Fig. 2b), is about 90 Å. As indicated by arrows in the figures, peaks of the films close to those coming from the (002) LAO and the (004) NGO reflections [18], are clearly visible at angles slightly smaller. They can be associated to values of the out-of-plane axis equal to 3.92 Å and 3.88 Å for film grown on LAO and NGO respectively. Thin films deposited in the same deposition run on STO did not show a peak well separated from that of the substrate. No peaks different from those of the substrates were

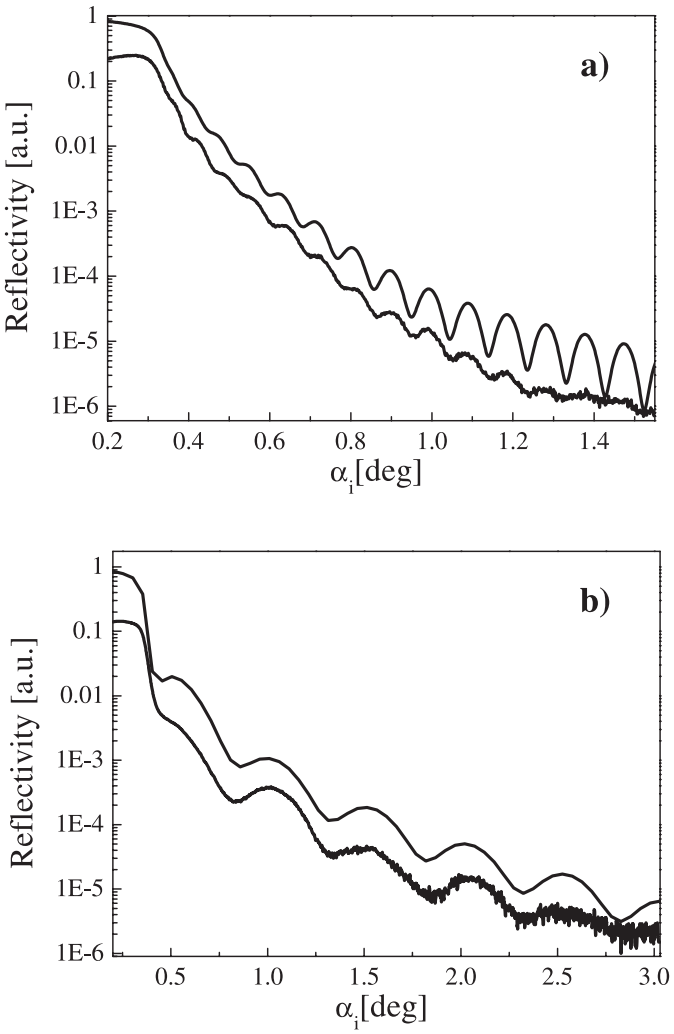


**Fig. 2.** a) Normalized small angle X-ray reflectivity measurement as a function of the incident angle for a $(La_{0.7}Sr_{0.3})_{0.6}MnO_3$ thin film deposited on STO (lower curve); the upper curve is the theoretical fit assuming a film thickness of 448 Å and an average surface roughness of 4 Å. b) Normalized small angle X-ray reflectivity measurement as a function of the incident angle for a $(La_{0.7}Sr_{0.3})_{1.3}MnO_3$ thin film deposited for a shorter time on NGO (lower curve); the upper curve is the theoretical fit assuming a film thickness of 87 Å and an average surface roughness of 3 Å. Experimental and theoretical curves are shifted one respect to the other for a better comparison between the two curves.

detectable on films deposited on STO, LAO and NGO, having thickness lower than about 90 Å. Typical full width at half maximum of the rocking curve for the (002) reflection (inset to Fig. 3a) was about 0.1°, another indication of the high quality of the samples. The $\phi$-scan measurements around the (103) asymmetric reflection, shown in Figure 4, performed on the same film in Figure 3a, points out the fourfold symmetry characteristic of the perovskite-like structure.

In Figure 5a, a typical behaviour of the electrical resistivity versus the temperature $\rho(T)$ curve for a sample

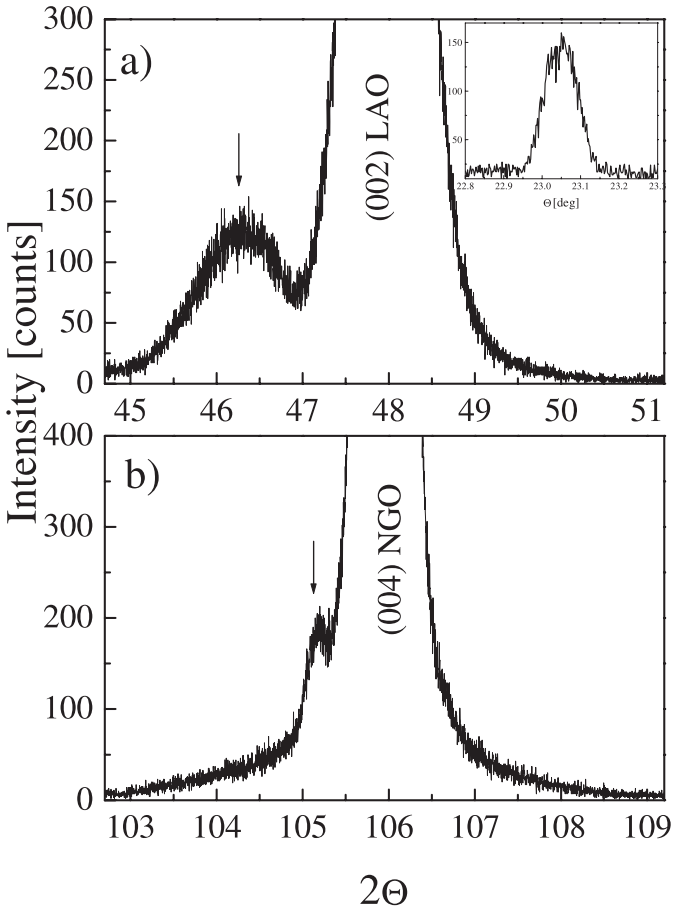


**Fig. 3.** X-ray diffraction spectra for $(La_{0.7}Sr_{0.3})_{1.3}MnO_3$ thin films about 90 Å thick grown on two different substrates: a) around the (002) reflection for the film grown on LAO; inset: rocking curve around the (002) reflection of the film. b) around the (004) reflection for the film grown on NGO. The arrows indicate peaks coming from the films. Both angular intervals are 6.5 degrees large for a better comparison between the two spectra.

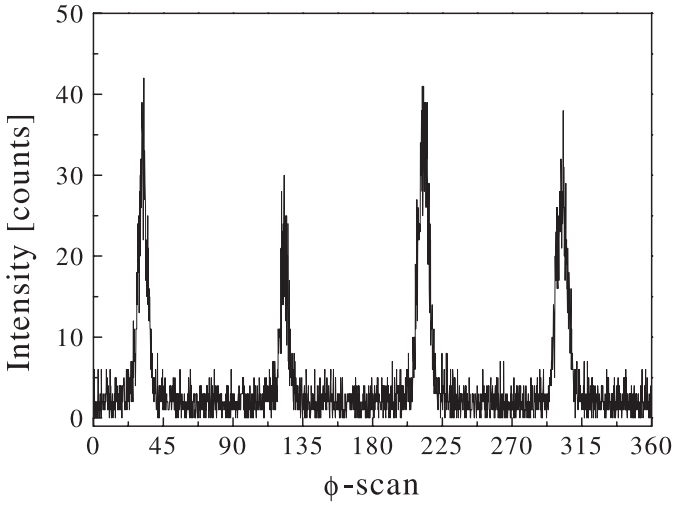


**Fig. 4.** $\phi$-scan measurement around the (103) reflection of 87 Å thick $(La_{0.7}Sr_{0.3})_{1.3}MnO_3$ thin film deposited on LAO substrate.

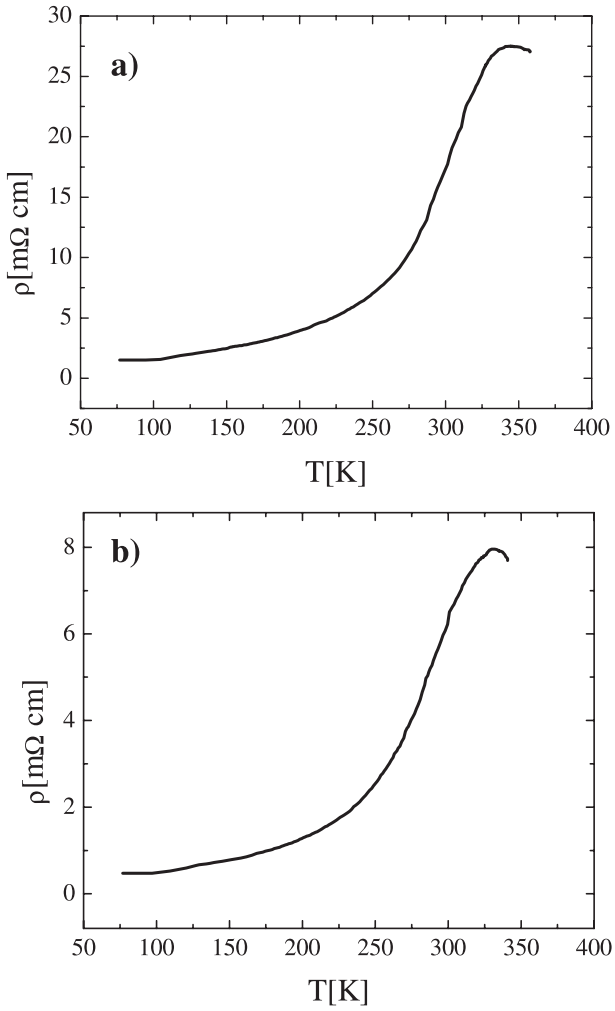


**Fig. 5.** a) Electrical resistivity $\rho$ versus the temperature $T$ curve for a typical $(La_{1-x}Sr_x)_yMnO_3$ thin film on STO about 400 Å thick. b) Electrical resistivity $\rho$ versus the temperature $T$ curve for a typical $(La_{1-x}Sr_x)_yMnO_3$ thin film on STO around 90 Å thick.

with a thickness of about 400 Å is shown. The transition from the high-temperature semiconductive to the low-temperature metallic behaviour is observed at the temperature $T_{MI} = 340$ K. The resistivity value in the zero temperature limit, $\rho = 1$ m$\Omega$ cm, is very close to values measured on single crystals with $x$ values close to 0.3, confirming the epitaxial quality of the films [19]. We point out that all the measured samples are as-grown films, which have not been subjected to any post deposition in situ or ex situ annealing process. In Figure 5b it is shown the $\rho(T)$ curve for a film around 90 Å thick with MI transition temperature $T_{MI} = 330$ K. These values are very close to those observed on bulk $La_{1-x}Sr_xMnO_3$ samples with $x = 0.3$ [20], and are a little surprising in as-grown very thin films with a not-optimised cationic stoichiometry. On the other hand, as outlined before, we point out the high non-accuracy of the EDS measurements and the important role that could be played by the oxygen stoichiometry in determining the actual doping level present

in the system. This role can be even enhanced in the case of thin films forced to grow with (La+Sr)/Mn ratios different from 1.

Oxygen stoichiometry plays a key role also in determining the relaxation of the lattice strain in manganite thin films [21–23]. In the case of $La_{0.7}Sr_{0.3}MnO_3$, it has been observed that the out-of-plane lattice constant on LAO substrates is decreased, while that on STO and NGO substrates is increased, with increasing the oxygen partial pressure during film growth by PLD [22]. The annealing in high oxygen pressure has been shown to produce the same effect, decreasing the out-of-plane lattice constant of $La_{0.7}Sr_{0.3}MnO_3$ films on LAO substrates [23].

We have also measured the $\rho(T)$ curves for epitaxial thin films grown in the same deposition run on different substrates (STO, LAO, NGO), to study the effects of the epitaxial strain on the MI transition and the metallic phase. In order to explain transport properties results only in terms of different epitaxial strains, it is fundamental to rule out spurious effects and to be assured of identical characteristics of the films, such as composition, doping level and thickness. In the case of our as grown films, obtained in the same deposition run without any post deposition annealing, this request is satisfied at the best. $\rho(T)$ results obtained on three films simultaneously deposited on NGO, Figure 6a, on STO, Figure 6b, and on LAO, Figure 6c, clearly indicated the effects of the strain on the MI transition temperature. The composition of the films in Figure 6 is $(La_{0.7}Sr_{0.3})_{0.8}MnO_3$ and their thickness is around 90 Å. The MI transition temperature for the film on NGO is $T_{MI} = 281$ K, while for the film on STO it is $T_{MI} = 265$ K and for that on LAO it is $T_{MI} = 243$ K. Moreover, the resistivity of the film grown on NGO (about 1 m$\Omega$ cm) is the lowest, and those of the films on STO and LAO are about one order of magnitude higher in the low temperatures limit. These results are in good agreement with the expectations based on the strength of epitaxial strain induced by the three kind of substrates employed, and, to our knowledge, are the first observed on as grown epitaxial films, without using pure ozone and with thickness below 100 Å.

As proposed by Millis and co-workers [24] the importance of the strain on the magneto transport properties of manganite films can be discussed in terms of two different effects. The uniform compression can increase the electron hopping probability, thus reducing the importance of the electron-lattice coupling. The opposite will happen in case of uniform expansion. Due to this "bulk" contribution, $T_{MI}$ variations can be either positive or negative depending on the nature of the biaxial strain if compressive or tensile. However, the second important strain effect is the biaxial distortion which increases the Jahn-Teller splitting of the $e_g$ electron levels. In this second case, the electrons can become much more localized and the $T_{MI}$ variations can be only negative. Consequently, the magneto transport properties will change as a function of the strain depending on which of the two effects is predominant. Our results show that a major role in the determination of the $\rho(T)$ behaviour is played by the strength of the strain

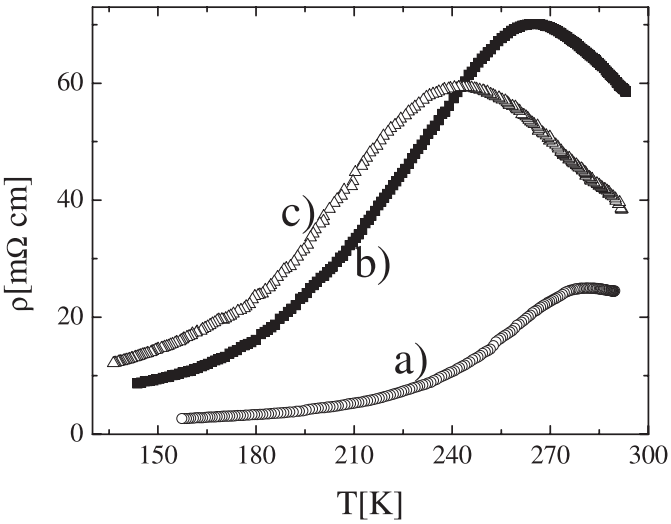


**Fig. 6.** Electrical resistivity $\rho$ versus the temperature $T$ curves for a series of $(La_{0.7}Sr_{0.3})_{0.8}MnO_3$ thin films, around 90 Å thick, deposited on a) NGO, b) STO and c) LAO.

present in the system, with the type of strain (compressive or tensile) being less important. More work is in progress to confirm these data and to study the $\rho(T)$ behaviour in the presence of an externally applied magnetic field.

The transport properties of the produced films have been periodically checked, and, independently by the care taken in their storing, resulted to be very stable, without appreciable changes over a period of about one year.

## 4 Conclusions

We have produced as grown $(La_{1-x}Sr_x)_yMnO_3$ epitaxial thin films using a MBE technique in which only low pressure of $O_2$+5% ozone, in the range of $10^{-5}$ torr, was present in the chamber during the deposition process. All the fabricated samples were not exposed to any in situ or ex situ annealing process after the growth. The films have been deposited on different substrates to measure and compare the structural and the transport properties of series of samples with different epitaxial strain obtained in the same deposition run. The structural properties of the films were analysed by RHEED analysis and XRD measurements and pointed out the production of high quality epitaxial films with surface roughness of the order of the interatomic distances and out-of-plane crystalline parameters influenced by the biaxial strain induced by the substrates. As grown samples, only 90 Å thick, have shown MI transition temperatures as high as 330 K, with resistivity values in the low temperatures limit very close to those observed on single crystals. Measurements of the $\rho(T)$ behaviour of thin films grown on different substrates in the same deposition run, clearly indicated the effects of the epitaxial strain on the MI transition temperature and the metallic phase. At a first glance, the strength of the biaxial strain seems to play a more important role with respect to the sign (tensile or compressive) of the strain.

The production of as grown epitaxial $(La_{1-x}Sr_x)_yMnO_3$ thin films with room temperature $T_{MI}$ transition using a deposition technique which allows the in situ control of the structural properties without introducing in the chamber highly corrosive gases and not requiring any in situ or ex situ annealing procedure, is of particular interest for carrying out more accurate studies about the influences of several parameters on the behaviour of manganite films. Moreover, the availability of a deposition procedure able to obtain as-grown manganite very thin films with atomically flat surfaces and high MI transition temperatures, will open new possibilities for microelectronic applications in which the production of multilayered systems is needed.

This work has been partially supported by the Research Project of National Interest (PRIN) "*Strain effects on the metal-insulator transition and on the metallic state of manganite thin films and heterostructures*" of the Italian Minister of the University and Research (MIUR). The authors gratefully acknowledge Dr. Alessandra Geddo Lehmann for discussing the X-ray measurements.

## References

1. K. Chahara, T. Ohno, M. Kasai, Y. Kozono, Appl. Phys. Lett. **63**, 1990 (1993); S. Jin, T.H. Tiefel, M. McCormack, H.M. O'Bryan, L.H. Chen, R. Ramesh, D. Schurig, Appl. Phys. Lett. **67**, 557 (1995); S.E. Lofland, S.M. Bhagat, H.L. Ju, G.C. Xiong, T. Venkatesan, L. Greene, S. Tyagi, J. Appl. Phys. **79**, 5166 (1996)
2. J. Fontcuberta, V. Laukhin, X. Obradors, Appl. Phys. Lett. **72**, 2607 (1998)
3. See for example, J.Z. Sun, D.W. Abraham, R.A. Rao, C.B. Eom, Appl. Phys. Lett. **74**, 3017 (1999); M. Bibes, L.I. Balcells, S. Valencia, S. Sena, B. Martinez, J. Fontcuberta, S. Nadolski, M. Wojcik, E. Jedrika, J. Appl. Phys. **89**, 6686 (2001), and references therein
4. P. Murugavel, J.H. Lee, J.-G. Yoon, T.W. Noh, J.-S. Chung, M. Heu, S. Yoon, Appl. Phys. Lett. **82**, 1908 (2003)
5. R. von Helmolt, J. Wecker, B. Holzapfel, L. Schultz, K. Samwer, Phys. Rev. Lett. **71**, 2331 (1993); K. Chahara, T. Ohno, M. Kasai, Y. Kozono, Appl. Phys. Lett. **63**, 1990 (1993); X.T. Zeng, H.K. Wong Appl. Phys. Lett. **66**, 3371, (1995); J. O'Donnell, M. Onellion, M.S. Rzchowski, J.N. Eckstein, I. Bozovic, Phys. Rev. B **54**, R6841 (1996)
6. M. Rajeswari, R. Shreekala, A. Goyal, S.E. Lofland, S.M. Bhagat, K. Ghosh, R.P. Sharma, R.L. Greene, R. Ramesh, T. Venkatesan, T. Boettcher, Appl. Phys. Lett. **73**, 2672 (1998); Z.-H. Wang, H. Kronmuller, O.I. Lebedev, G.M. Gross, F.S. Razavi, H.-U. Habermeier, B.G. Shen, Phys. Rev. B **65**, 054411 (2002)
7. J.N. Eckstein, I. Bozovic, J. O'Donnell, M. Onellion, M.S. Rzchowski, Appl. Phys. Lett. **69**, 1312 (1996)
8. D.D. Berkeley, B.R. Johnson, N. Anand, K.M. Beauchamp, L.E. Conroy, A.M. Goldman, J. Maps, K. Mauersberger, L.M. Mecartney, J. Morton, M. Tuominen, Y.-J. Zhang, Appl. Phys. Lett. **53**, 1973 (1988)
9. S. Kaneko, U. Hiller, J.M. Slaughter, C.M. Falco, C. Coccorese, L. Maritato, Phys. Rev. B **58**, 8229 (1998)
10. B.A. Joyce, J.H. Neave, P.J. Dobson, P.K. Larsen, Phys. Rev. B **29**, 814 (1984)
11. J. O'Donnell, A.E. Andrus, S. Oh, E.V. Colla, J.N. Eckstein, Appl. Phys. Lett. **76**, 1914 (2000)
12. S. Valencia, L.I. Balcells, J. Fontcuberta, B. Martinez, Appl. Phys. Lett. **82**, 4531 (2003)
13. See for example *Colossal Magneto-Resistance Oxides. Monograph in Condensed Matter Science*, edited by Y. Tokura (Gordon & Branch, New York, 2000) and references therein
14. Y. Wu, Y. Suzuki, U. Rüdiger, J. Yu, A.D. Kent, T.K. Nath, C.B. Eom, Appl. Phys. Lett. **75**, 2295 (1999)
15. P.G. Radaelli, G. Iannone, M. Marezio, H.Y. Hwang, S.-W. Cheong, J.D. Jorgensen, D.N. Argyriou, Phys. Rev. B **56**, 8265 (1997)
16. A.M. Haghiri-Gosnet, J. Wolfman, B. Mercey, Ch. Simon, P. Lecoeur, M. Korzenski, M. Hervieu, R. Desfeux, G. Baldinozzi, J. Appl. Phys. **88**, 4257 (2000)
17. A.M. Haghiri-Gosnet, J.P. Renard, J. Phys. D **36**, R127 (2003)
18. J. Dho, Y.N. Kim, Y.S. Hwang, J.C. Kim, N.H. Hur, Appl. Phys. Lett. **82**, 1434 (2003)
19. R. Shiozaki, K. Takenaka, Y. Sawaki, S. Sugai, Phys. Rev. B **63**, 184419 (2001)
20. See for example, J. Coey, M. Viret, S. Von Molnar, Adv. Phys. **48**, 167 (1999); M.B. Salamon, M. Jaime, Rev. Mod. Phys. **73**, 583 (2001)
21. M. Rajeswari, R. Shreekala, A. Goyal, S.E. Lofland, S.M. Bhagat, K. Ghosh, R.P. Sharma, R.L. Greene, R. Ramesh, T. Venkatesa, T. Boettcher, Appl. Phys. Lett. **73**, 2672 (1998)
22. J. Dho, N.H. Hur, I.S. Kim, Y.K. Park, J. Appl. Phys. **94**, 7670 (2003)
23. K.M. Krisham, H.L. Ju, Phys. Rev. B **60**, 14793 (1999)
24. A.J. Millis, T. Darling, A. Migliori, J. Appl. Phys. **83**, 1588 (1998)